Received: 17 September 2018 | Revised and accepted: 20 November 2018

DOI: 10.1002/mmce.21630

WILEY INTERNATIONAL JOURNAL OF RF AND MICROWAVE COMPUTER-AIDED ENGINEERING

RESEARCH ARTICLE

Polarization independent broadband metamaterial absorber for microwave applications

Mehmet Bağmancı[1] | Oğuzhan Akgöl[1] | Melikşah Özaktürk[2] | Muharrem Karaaslan[1] | Emin Ünal[1] | Mehmet Bakır[3]

[1]Department of Electrical and Electronics Engineering, Iskenderun Technical University, Iskenderun, Hatay, Turkey

[2]Department of Energy Systems Engineering, Iskenderun Technical University, Iskenderun, Hatay, Turkey

[3]Faculty of Engineering and Architecture, Department of Computer Engineering, Bozok University, Yozgat, Turkey

Correspondence
Mehmet Bakır, Faculty of Engineering and Architecture, Department of Computer Engineering, Bozok University, Yozgat, Turkey.
Email: mehmet.bakir@bozok.edu.tr

Abstract

A new polarization independent broadband metamaterial absorber (MA) structure based on split ring resonators which are loaded with lumped elements and via connection lines is proposed. The designed structure shows a perfect absorption between 4 and 16 GHz which is validated by simulation studies. Experimental study is only made for the structure that has no via connections and no the lumped element resistors to show the importance of these entities in the proposed metamaterial structure. Both numerical and experimental study results show that broadband MA property depends on the resistors and via connections on the proposed structure. By having high absorption in a wideband range which is numerically demonstrated, the proposed structure can be used in energy harvesting or wireless power transfer applications with higher efficiencies.

KEYWORDS

absorber, broadband, metamaterial

1 | INTRODUCTION

Metamaterials have attracted great attention owing to their unique electromagnetic and optical properties, such as negative refraction[1] and asymmetrical transmission.[2–4] One of the most popular types of metamaterial is metamaterial absorbers (MA) which was initially proposed by Landy et al.[5] in 2008. After that, different types of single band and multi band MA studies were proposed.[6,7] In addition, polarization independent and tunable perfect metamaterial absorbers (PMA) with wide incidence angles were designed in microwave, THz, and optical frequency bands.[8–10]

Because of the diffraction limitations, traditional absorbers cannot be designed and produced in small dimensions. Since reduction in the electrical thickness of the absorbers is one of the main design inputs, the need for producing these absorbers has emerged. Tao et al. realized a study in which they achieved 96% absorption at 1.6 THz.[11]

Metamaterials are also used in many areas including super lenses,[12] invisibility cloaking,[13,14] polarization rotation,[15] sensing applications,[16] antennas and energy harvesting.[17–21] Researchers have been working on bandwidth enhancement and polarization insensitiveness by applying different methods.[22–24] These methods can be listed as resistive film placement, loading lumped elements, and using multilayer structures.[25–30] In a study conducted by Tang et al.,[25] resistive films which were vertically placed on the metal plate were used to increase the bandwidth. In that study, polarization independent MA was designed and its operation between 20 and 55 GHz is demonstrated. In Ref. 26, Mulla et al. obtained a bandwidth increase by using multilayer structure numerically between 624 and 658 THz. Chen et al. designed MA which was composed of a single dielectric substrate, double circular metallic rings and resistive loads operating between 8.87 and 16.47 GHz. In Ref. 27, Chen et al. studied a broadband absorber by using lumped elements and they obtained more than 7 GHz bandwidth with 90% absorption. In Ref. 28, Ding et al. conducted a study for a microwave ultra-broadband polarization independent metamaterial by using periodic array of metal-dielectric quadrangular frustum pyramids between 7.8 and 14.7 GHz. In Ref. 29, Ma et al. realized a broadband absorber using the fractal tree structure which

consists of three metallic layers separated by two dielectric substrates that is operating between 4.98 and 12.58 GHz. In Ref. 30, Cheng et al. realized a wide-band metamaterial absorber, based on fractal frequency selective surface and resistive films. They demonstrated a wideband absorber between 6.51 and 25.42 GHz by using Minkowski fractal loop structure and Ohmic loss properties of resistive films numerically.

In this study, we have used a multilayered structure that is composed of three metallic layers which are separated by two dielectric layers. Metallic layers on the top and middle parts consist of split ring cross ring resonators. On the top layer, resistive loads are placed between the splits of resonators as well as three metallic layers connected by metallic connections with each other. Operation frequency is chosen between 4 and 16 GHz to cover most critical applications. In order to achieve polarization and incident angle insensitive operation the proposed structure is realized by considering a symmetrical design.[31,32] Organization of the study is as follows; design and numerical setup is explained in section two and numerical simulations is demonstrated in section three to demonstrate operation of the proposed broadband MA. In order to support the numerical results, experimental study is presented in section four and the study is concluded in section five.

2 | DESIGN OF THE MA UNIT CELL AND THE NUMERICAL SETUP

Design of the proposed broadband perfect MA unit cell is shown in Figure 1. Unit cell design is composed of three layers, which are placed at the top, middle and back side of the structure as shown in Figure 1A-C, respectively. There are two dielectric layers which are composed of FR4 with a thickness of 1.6 mm. Dielectric constant and loss tangent values of FR4 substrate are $\varepsilon_r = 4.3$, $\tan\delta = 0.025$, respectively. There are metallic circular connections between the top and middle layer resonators at four points as shown in the Figure 1A. Diameter of the metallic connection is 0.6 mm and it is also made of copper element. Resonators, connections and back layer are also constructed with copper that has a conductivity of 5.8×10^7s/m. The thickness of the resonator as well as the back copper layer is 0.035 mm which is given in the Table 1 along with the dimension details of the proposed structure. All of three metallic layers are connected with copper connectors.

TABLE 1 Typical size of proposed structure

Parameter	*a*	*r*	*w*	*g*	*k*	*l*	*t*
Value (mm)	12	4.1	0.6	1	0.5	7.6	1.6
Other	Metallic layers' thickness: 0.035 mm						
	Connector' radius: 0.3 mm, resistors value: 220 Ω						

These dimensions are optimized for the best numerical results, while unit cell boundary conditions are applied along $-x$ and $-y$ direction, open add space boundary is applied along $+z$ direction and the wave is incident along $-z$ direction in TE and TM mode simulations as shown in Figure 2A. CST Microwave Studio based on Finite integration technique (FIT) is used for numerical analysis. The boundaries in CST are defined as *unit cell*, *unit cell*, Open Add Space along *x*, *y*, and *z* axes, respectively. Periodic boundaries are chosen for easy applications. A novel geometry was specifically designed for broadband MA applications by having self and mutual coupling effects. For this reason, this unique design is created for enhancing coupling effects of the resonators to provide broadband MA properties. PEC, PMC boundary conditions are applied for the simulation of TEM mode as shown in Figure 2B.

3 | NUMERICAL SIMULATIONS

One of the most important requirements of an absorber is to confine the penetrated energy within the structure. Reflected and transmitted waves have to be minimized to obtain perfect absorption. Electromagnetic simulations and the theoretical diffraction efficiency were predicted from a full wave electromagnetic simulator that includes all the geometrical and material aspects of the proposed structures. Unit cell boundary conditions were chosen for *x*–*y* plane and open (add space) for *z* direction. The theoretical diffraction efficiency was predicted from full-wave numerical simulations (that include all geometrical and material aspects of the fabricated structures). In order to understand the absorption characteristics of the proposed structure, some numerical simulations are also performed.

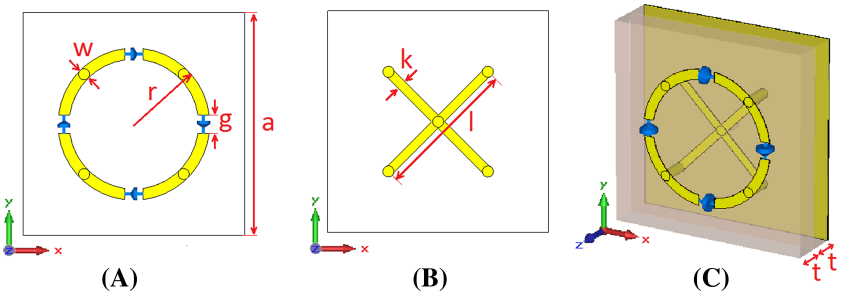

FIGURE 1 The geometry of unit-cell PMA (A) top metallic layer and first substrate, (B) middle metallic layer and second substrate, (C) side view of structure

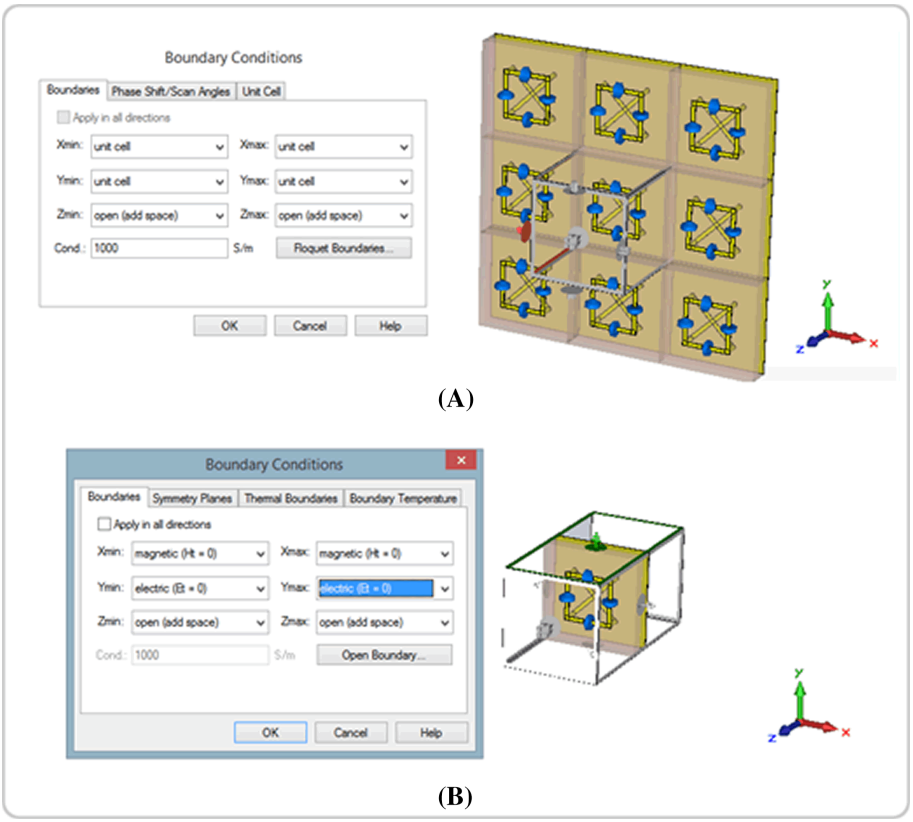

FIGURE 2 Boundary setup of CST microwave studio, (A) unit cell boundary setup for TE and TM modes, (B) PEC-PMC boundary setup for TEM mode

Absorption response $[A(\omega)]$ of PMA in terms of frequency can be calculated by using the following equations in which no higher order diffraction is considered due to good wavelength characterization of the proposed structure.

$$A(w) = 1 - R(w) - T(w) \tag{1}$$

$$R(w) = |S_{11}|^2 \tag{2}$$

$$T(w) = |S_{21}|^2 \tag{3}$$

Equivalent of R_w and T_w is given in Equations (2) and (3) where S_{11}, S_{21} denote the scattering parameters in terms of reflected and transmitted powers. In order to increase absorption (A_w) to a higher level, both reflection and transmission have to be minimized. When we look at these equations, it can be easily seen that the dispersive parameters of dielectric layer is directly affecting the incident and transmitted waves. Since the back layer is completely covered with copper, transmitted wave is going to be so small that it can be assumed as zero and it would be negligible. After that, $A(w)$ can be assumed to be found as in the following equation;

$$\mathrm{A}(w) = 1 - R(w) = 1 - |S_{11}|^2 \tag{4}$$

In order to give more details about the proposed broadband MA, TE, and TM mode simulation results, electrical field, magnetic field, and surface current distributions and polarization together with incident wave angle independency topics are explained in the following sections.

3.1 | Broadband absorber characteristics in TE and TM mode

In order to explain the proposed broadband MA characteristics, A(w) and S_{11} parameter are numerically analyzed by using CST microwave studio. As explained before, unit cell boundary conditions are chosen for the demonstration of TE and TM mode between 4 and 16 GHz. When we look at the numerical analysis results of A(w) and S_{11}which is given in Figure 3, we can see the perfect absorption between 6.2 and 13.5 GHz which means that the total absorption bandwidth is about 7.3 GHz. This bandwidth is bigger than the absorption bandwidth in Ref. 24 which was obtained by films. As explained before, this bandwidth is obtained by using lumped element and multilayer structured design in the proposed MA. According to simulation results 67% absorption achieved with respect to whole bandwidth which is 12 GHz between 4 and 16 GHz.

In order to explain the physical behavior of the proposed broadband MA, electric field, magnetic field, and surface current distributions are examined at the resonance frequency of 6.82 and 12.72 GHz. These frequencies are particularly chosen because the absorption values are in their maximum levels at these points. Corresponding absorption values are 95.29 % and 97.61 % , respectively. Electric field is concentrated at the left and right side of the split ring resonator according to the electrical field direction for the top layer as shown in Figure 4A. In the middle layer, electric field is concentrated at the left and right side of the metallic patches in

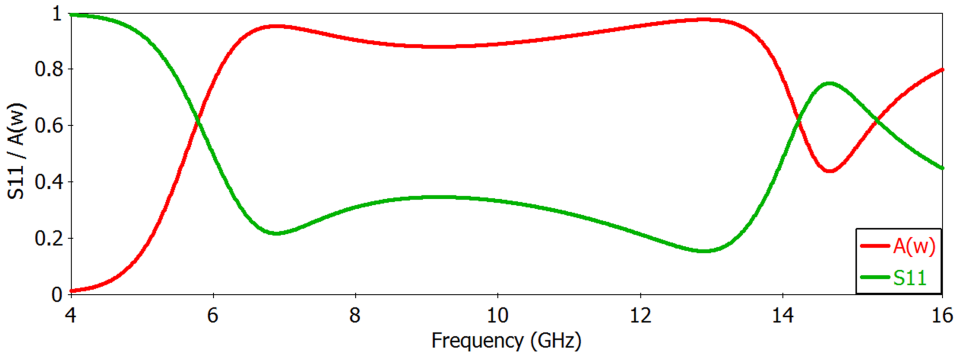

FIGURE 3 Reflection coefficient and absorption magnitude of perfect metamaterial absorber

accordance with the electric field direction. When we examine the electrical field at 12.72 GHz, while electrical field at the top layer is concentrated at the left and right side of the split ring resonator, electrical field is intensively concentrated on the top and bottom sides of the metallic patches. We can say according to this figure that the second resonance of the proposed structure is caused by middle layer and connectors between the middle layer and top layer. When we look at the magnetic field distribution, we can see compatible results in accordance with the electrical field distribution results. This is because of the connection between the top and middle layer resonators. When we look at Figure 3C, parallel and anti-parallel surface currents can be seen. While parallel currents excite an electric field, the anti-parallel currents excite a magnetic field. These responses couple with E and H components of the incident EM wave and produce a strong localized EM field at the resonance frequency.

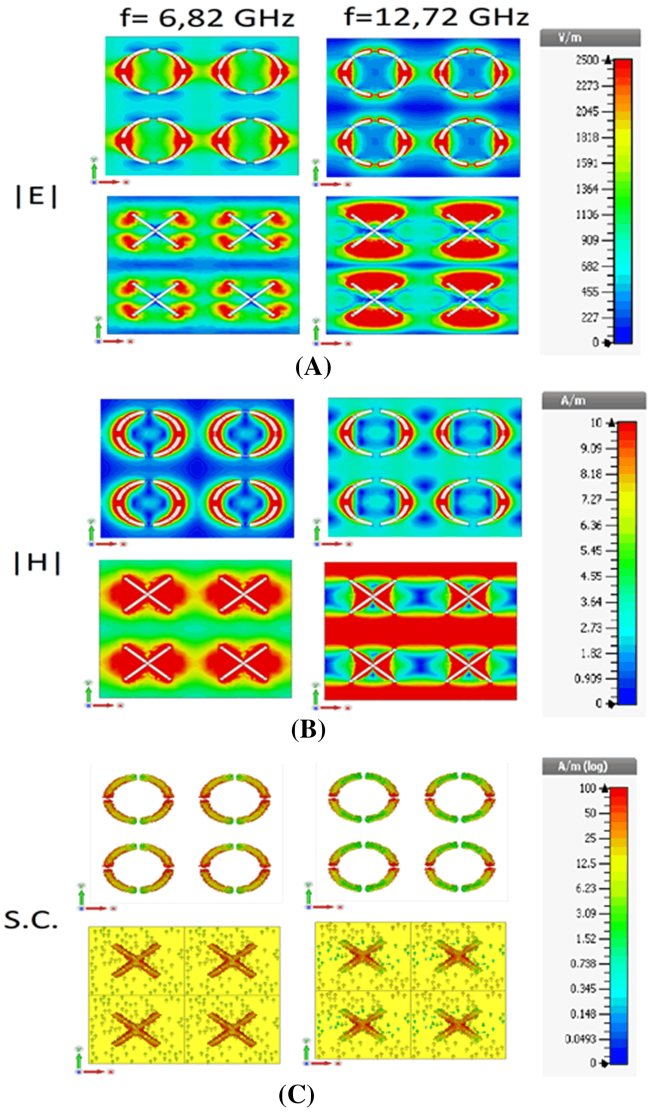

FIGURE 4 Electric field distribution (A), magnetic field distribution (B) and current distribution of PMA for circle resonator and cross resonator separately for 6.82 and 12.72 GHz. (C) Surface current

3.2 | Absorption in different polarizations and angles

Polarization and incident angle independency topics are important for absorber applications to show the same properties in different modes. In order to investigate this feature, CST microwave studio is used for numerical analysis for showing TE, TM, and TEM mode absorption characteristics. In Figure 5, numerical analysis results for absorption in TE, TM, and TEM modes are presented. TE and TM mode absorption graphics are similar due to the symmetrical design of the proposed structure. The achieved absorption value is higher than 80% between 6.2 and 13.5 GHz. Absorption value is also higher than 80% in the given frequency band, but small decreases occurred at around 12 GHz in TEM mode. Numerical simulation results showed that the proposed broadband MA presents a good absorption compared with the similar studies in current literature[23,24] for C, X, and Ku band applications.

In order to investigate polarization angle and incident angle characteristics in TE, TM, and TEM mode applications of the proposed broadband metamaterial absorber, numerical simulations are completed and presented in Figure 6. As shown in Figure 6A,B, when polarization angle has been changed, no big difference occurred between 6.2 and 13.5 GHz. Absorption value is higher than 80% in the given frequency band when polarization angle is changed in TE and TM modes. In TEM mode, incident angle changes result in with no change in the absorption due to the symmetrical design of the proposed structure (Figure 6C). Numerical results showed that the proposed broadband MA maintains

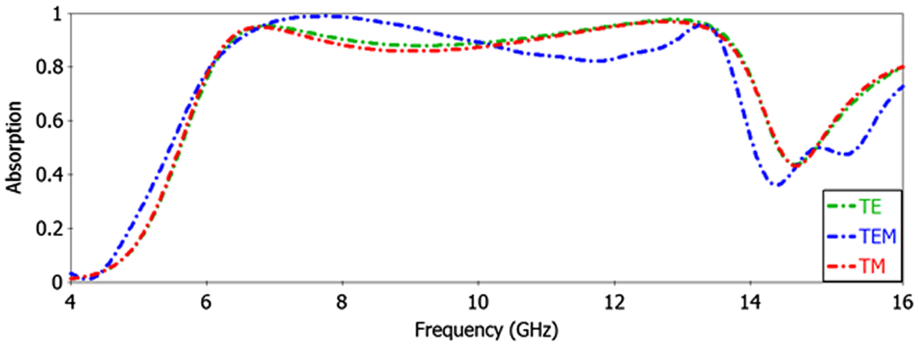

FIGURE 5 Absorption characteristic of PMA for TE and TM polarization and TEM mode

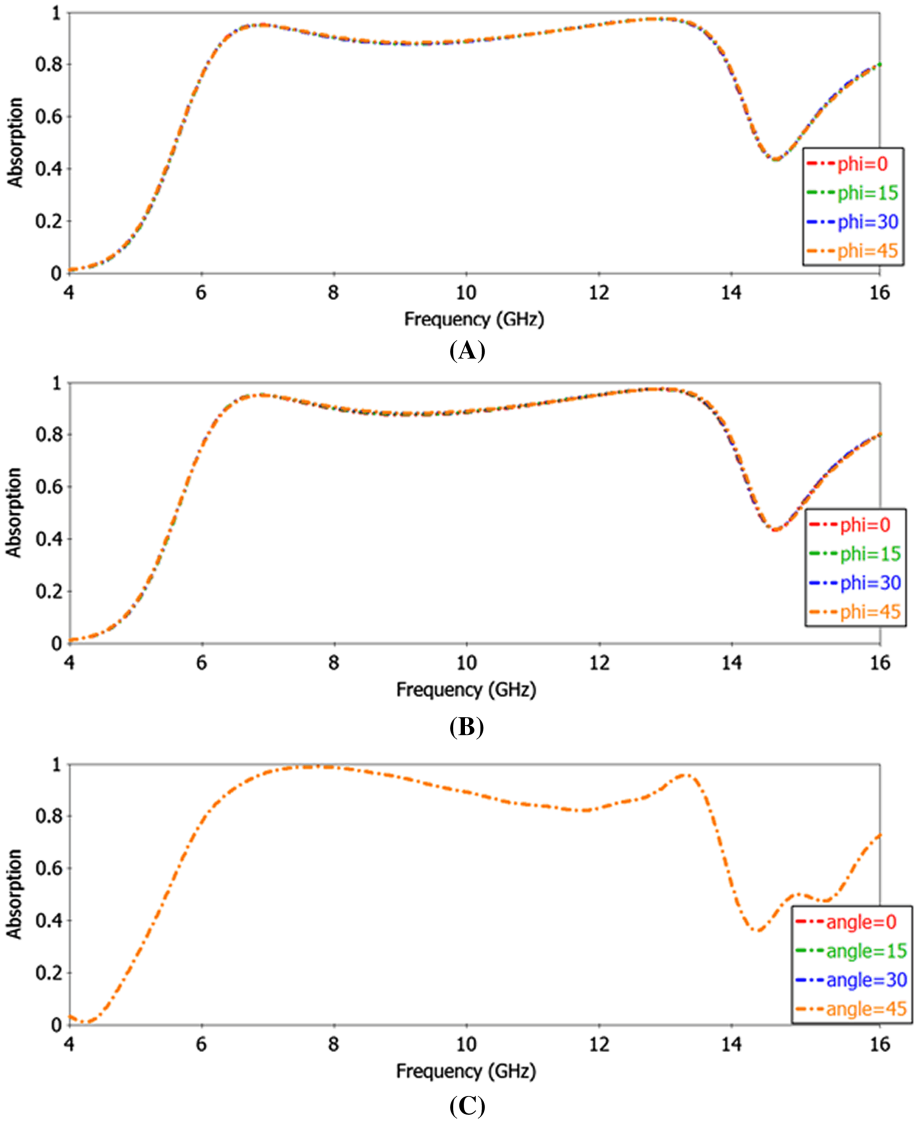

FIGURE 6 Absorption response of the proposed PMA for different angles of incident wave (a) phi angle for TE polarization (B) phi angle for TM polarization and (C)TEM mode

its absorption characteristics in terms of polarization and incident angle changes in all of TE, TM, and TEM mode applications in the given frequency band. These numerical results also show that this application can be used in energy harvesting applications since the obtained perfect absorption is independent from polarization and wave modes.

3.3 | Absorption in different design parameters

In order to show the effects of design parameters in absorption values in a given frequency band, some design parameters have been investigated by using CST Microwave Studio's parametric sweep function. TE mode has been chosen for illustration in this part of the study and unit cell

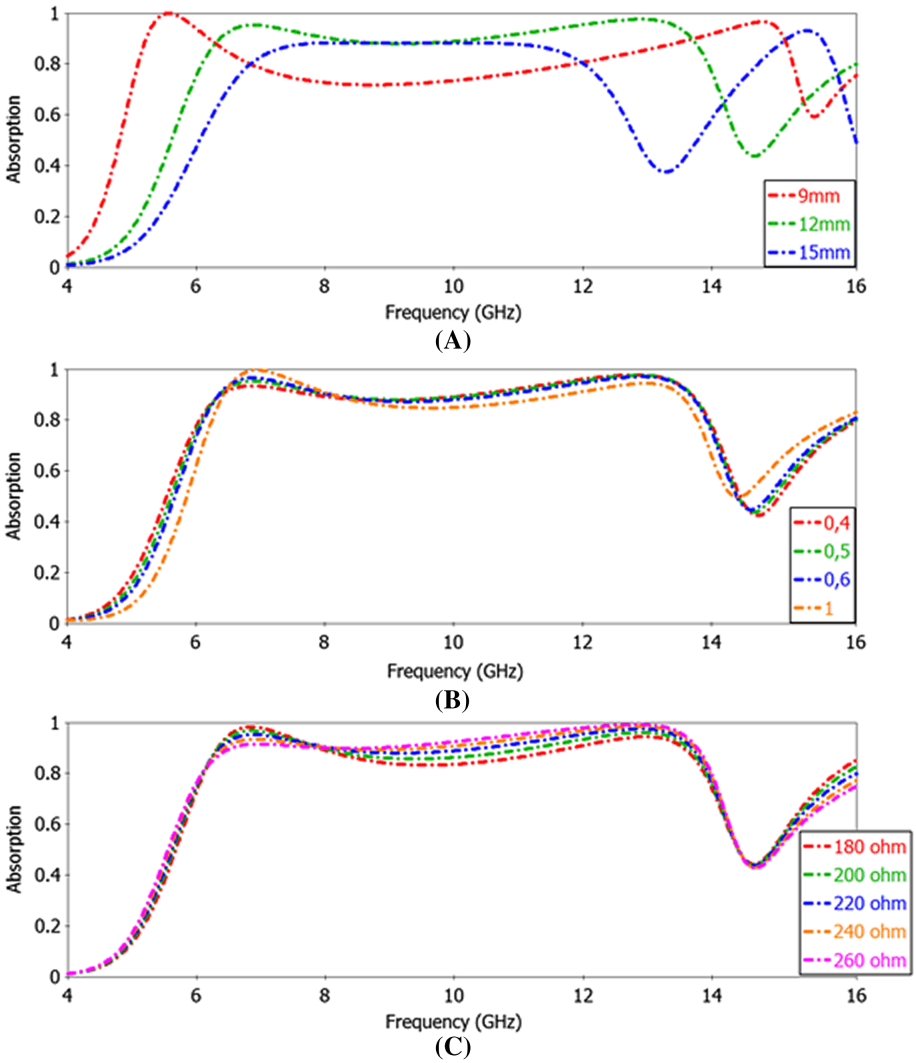

FIGURE 7 The absorption response of the proposed wideband MA in different line width and length of the substrate (A), line-width of cross resonator, (B) and different resistance values of the lumped resistors (C)

boundary conditions have been used to do so. First of all, substrate length which is characterized as "*a*" in Figure 1A is changed between 9 and 15 mm and the corresponding absorption results are presented in Figure 7A. Although bandwidth increases when 9 mm is chosen as an example, the absorption value decreases dramatically lower than 80%. When 15 mm substrate length is chosen, bandwidth and absorption values also decrease to 4 GHz and 80%. It is worth to remark that the absorption value is almost constant between 7.5 and 11.5 GHz in this case. As shown in the figure, optimum results are obtained when the substrate length is adjusted as 12 mm and explains why 12 mm is selected as the substrate length for the proposed broadband MA.

As a second demonstration, line width of cross resonator which is placed in the middle layer and characterized as "k" in Figure 1A was chosen. This parameter has been changed between 0.4 and 1 mm with the increment of 0.2 mm. As shown in Figure 7B, the line width of the cross resonator does not affect the absorption value as substrate width. Similar absorption characteristics are obtained when the line width has been changed between 0.4 and 1 mm. For this reason, 0.5 mm is used in the proposed broadband metamaterial absorber.

Finally, the resistance value which is used as a lumped element between the splits of resonator in the top layer has been changed from 180 to 260 Ω with 20 Ω steps. As shown in Figure 7C, the absorption bandwidth remains stable in a given frequency band, except for the first but small changes that occurred in the middle frequency band. Optimum results are obtained with 220 Ω resistor value and that is why this value is chosen in the proposed broadband MA.

3.4 | Investigation of the effects of metallic patches and lumped elements in absorption

In order to show the effects of metallic patches which connect the top and middle layer resonators in the proposed broadband MA, absorption characteristics in TE mode, with and without these metallic patches were numerically analyzed. As shown in Figure 8A, patches connecting top and middle layer resonators play an important role in the

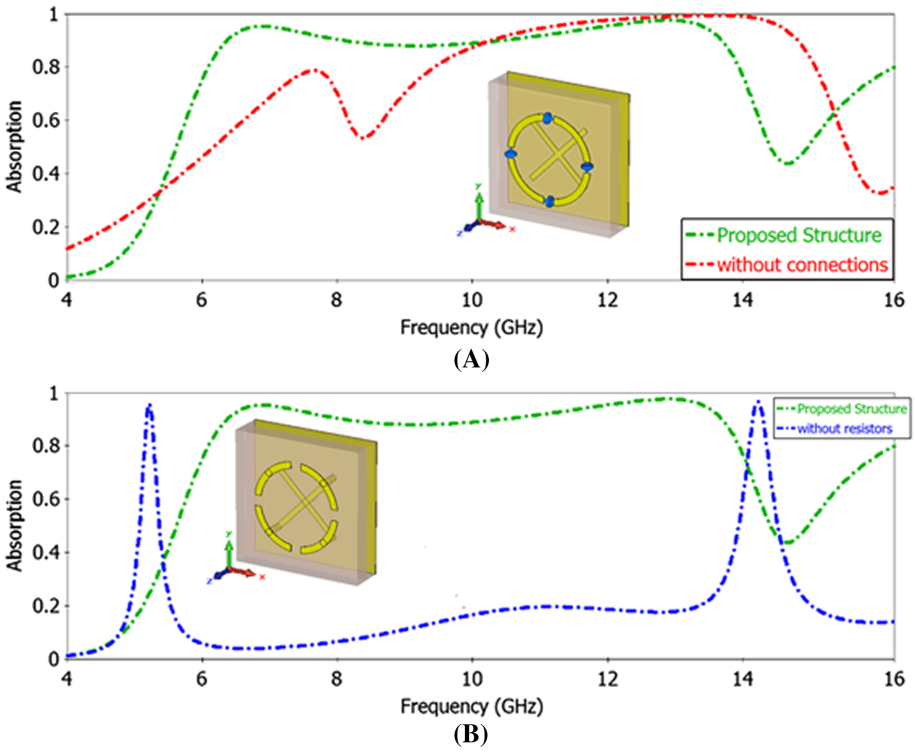

FIGURE 8 Absorption response of the proposed structure and without connections (A), without resistors (B) and without connections and resistors

absorption bandwidth. When no patch is used, absorption occurs between 10.5 and 15 GHz which means that the absorption bandwidth decreases from 7.3 to 4.5 GHz. Furthermore, absorption frequency shifted to 10.5 GHz meaning that the absorption in lower X band and upper C band is not possible if the connectors are not used. Furthermore, absorption magnitudes at the resonance frequency of 6.2 and 13.5 GHz become 95.9%and 96.7%, respectively. According to the numerical simulation results, it is clear that the connectors are playing an important role in both absorption and bandwidth.

In order to show the effects of resistors used on the splits of resonators on the top layer, absorption magnitude is compared with the situation in which no resistor was used on that splits. Absorption characteristics are compered in TE mode excitation and numerical simulation results are presented in Figure 8B. As shown in the figure, resistors are crucial in the absorption bandwidth since no absorption occurs between 6.2 and 13.5 GHz if resistors are not used. Resonance frequencies are 5.2 and 14 GHz while the bandwidth is about 150 MHz in these frequencies. According to the figure, when 220 Ω resistors are used as lumped elements in the proposed broadband MA, absorption bandwidth becomes 45 times bigger than that of the situation without any lumped element.

4 | FABRICATION AND MEASUREMENT

In order to support the numerical simulation results with experimental data, we have manufactured and measured the proposed structure without resistors and connectors between

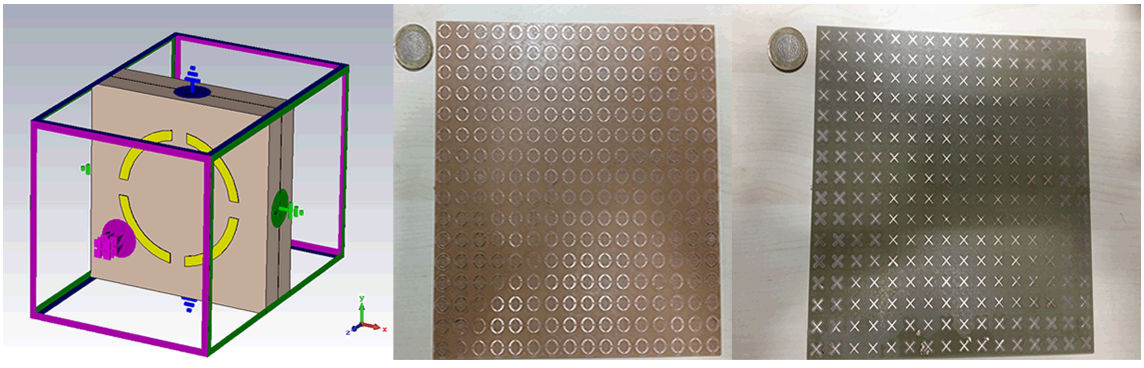

FIGURE 9 A, Simulation setup for experimental validation; B, fabricated middle layer; C, fabricated top layer

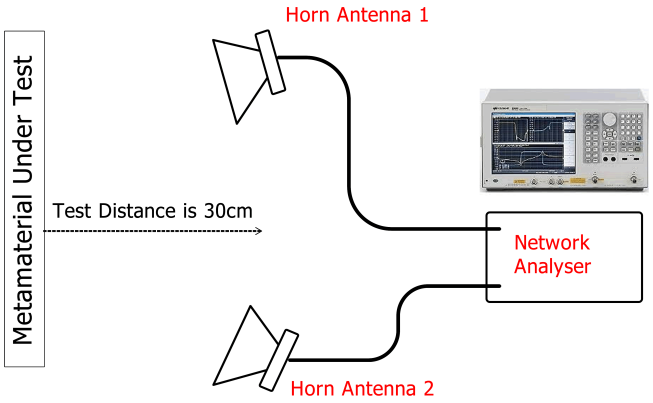

FIGURE 10 Experimental setup for absorption measurement

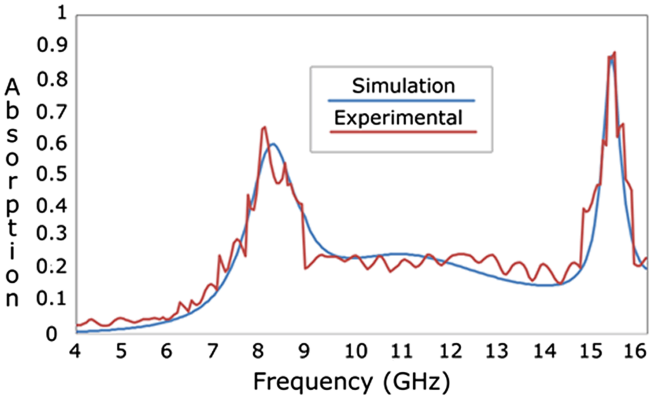

FIGURE 11 Experimental and simulation absorption value comparison when no patch and no lumped resistors used in the proposed broadband MA between 4 and 16 GHz

the top and middle layers as shown in Figure 9A. Top and middle resonator layers are composed of 16 × 16 unit cells and fabricated by using LPKF E33 CNC controlled PCB production machine as shown in Figure 9B,C. Unfortunately, copper planes without numerous perforations are impossible since in practice without using micro via PCB production technique. Simply connecting resistors from external conductor to a PCB's reference plane can encourage external noise currents to flow through the plane and it can increase the RF currents from output drivers. Due to these disadvantages and having insufficient fabrication techniques in our laboratory, we have fabricated the proposed structure without via and without resistor connection as presented in Figure 9B,C.

The CST simulations were carried out under plane wave incidence, concerning the measurement results and simulation results compatibility as shown in Figure 11. We set the test distance to 30 cm which is four times greater than the minimum wavelength as schematically given in Figure 10.

Structure without metallic connections and resistive loads is fabricated as mentioned in the previous sections. The reason is that it is difficult to join the copper layers via copper connections and solder the resistors on circle resonators. Fabricated structure is demonstrated in Figure 9A. Length and width of the structure are both 19.2 mm. The structure is composed of 256 unit-cells (16 × 16). First and second layers are demonstrated in Figure 9B,C, respectively. Measurements are realized by means of Agilent N5234A PNA-L Microwave Network Analyzer. When we look at Figure 11, simulation and experimental tests results seem to be compatible with each other except for small differences caused by the calibration errors and non-perfect testing equipment. As explained before, resistors are playing an important role in the bandwidth of the proposed broadband MA, experimental and simulation data verify this conclusion. In addition, connectors, as explained before, affect the absorption frequencies, thus when no connectors are used, the absorption frequencies become 8 and 15.5 GHz. This is because of the inductive effects of the connectors; resonance frequencies occur in higher frequencies due to the decrease occurred in the inductance of metallic elements.

Finally, energy harvesting performance of the proposed structure has been simulated when incident power is set to 0.5 W in the electromagnetic simulation program. Simulated energy harvesting value between 6.8 and 12.8 GHz is 0.43 W which corresponds to 86% of the incident electromagnetic energy as shown in the Figure 12 as a loss in lumped elements. According to this figure it can be said that the most of the incident electromagnetic energy loss is on the FR-4 substrate.

Another important topic which is related with energy harvesting is RF to DC conversion efficiency which can be

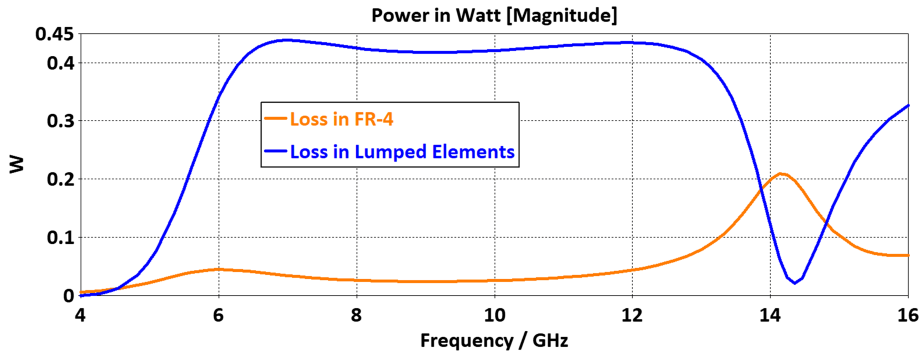

FIGURE 12 Simulated energy harvesting characteristics of the proposed structure between 4 and 16 GHz

defined as PDC/PRF. There are several studies conducted in current literature regarding to RF to DC efficiency in MA as in Ref. 33. According to the cited study, almost 76% of the incident electromagnetic wave energy can be converted to dc energy when −5 db power is obtained.

5 | CONCLUSION

This study focuses on the broadband metamaterial absorber by using a multilayer structure. Proposed structure is composed of split ring resonators, cross resonators and resistors. A unique design is created by using numerical study which is also experimentally tested to support the obtained numerical data. Effects of the metallic connectors and resistors of the working mechanism are investigated numerically. Operation of the broadband MA is explained by using electric field, magnetic field and surface current distributions. Numerical results show that this structure maintains 7.3 GHz bandwidth between 4 and 16 GHz in different modes and different incident angles which is crucial in the absorber applications. Furthermore simulated energy harvesting performance is over 83% between 6.8 and 12.8 GHz.

ORCID

Muharrem Karaaslan https://orcid.org/0000-0002-4661-1267
Mehmet Bakır https://orcid.org/0000-0002-5847-743X

REFERENCES

1. Shelby RA, Smith DR, Schultz S. Experimental verification of a negative index of refraction. *Science*. 2001;292:77-79.
2. Dincer F, Sabah C, Karaaslan M, Unal E, Bakir M, Erdiven U. Asymmetric transmission of linearly polarized waves and dynamically wave rotation using chiral metamaterial. *Prog Electromagn Res*. 2013;140:227-239.
3. Ozer Z, Dincer F, Karaaslan M, Akgol O. Asymmetric transmission of linearly polarized light through dynamic chiral metamaterials in a frequency regime of gigahertz–terahertz. *Opt Eng*. 2014;53(7):075109-075109.
4. Dincer F, Karaaslan M, Akgol O, Unal E, Sabah C. Asymmetric transmission of linearly polarized electromagnetic waves using chiral metamaterials with constant chirality over a certain frequency band. *Mod Phys Lett B*. 2014;28(32):1450250.
5. Landy NI, Sajuyigbe S, Mock JJ, Smith DR, Padilla WJ. Perfect metamaterial absorber. *Phys Rev Lett*. 2008;100:207402.
6. Dincer F, Karaaslan M, Unal E, Delihacioglu K, Sabah C. Design of polarization and incident angle insensitive dual-band metamaterial absorber based on isotropic resonators. *Prog Electromagn Res*. 2014;144:123-132.
7. Bakir M, Karaaslan M, Dincer F, Delihacioglu K, Sabah C. Perfect metamaterial absorber-based energy harvesting and sensor applications in the industrial, scientific, and medical band. *Opt Eng*. 2015;54(9):097102.
8. Durmaz F, Li Y, Arif EC. A multiple-band perfect absorber for SEIRA applications. *Sens Actuators B*. 2018;275:174-179.
9. Mulla B, Sabah C. Ultrathin thermally stable multiband metamaterial absorber design for solar energy applications. *J Nanophoton*. 2018;12(1):016005.
10. Bakır M, Karaaslan M, Dincer F, Delihacıoğlu K, Sabah C. *J Mater Sci Mater Electron*. 2016;27:12091.
11. Padilla WJ, Averitt RD. Highly flexible wide angle of incidence terahertz metamaterial absorber:design, fabrication, and characterization. *Phys Rev B*. 2008;78(24):241103.
12. Garcia N, Vesperinas M. Left-handed materials do not make a perfect lens. *Phys Rev Lett*. 2008;88(20):207403.
13. Steven A, Popa BL, Schurig D, et al. Full-wave simulations of electromagnetic cloaking structures. *Phys Rev E*. 2006;74(3):036621.
14. Cai W, Chettiar UK, Kildishev AV, et al. Optical cloaking with metamaterials. *Nat Photon*. 2007;1(4):224-227.
15. Kwon DH, Pingjuan LW, Douglas HW. Optical planar chiral metamaterial designs for strong circular dichroism and polarization rotation. *Opt Exp*. 2008;16:11802-11807.
16. Karaaslan M, Bakir M. Chiral metamaterial based multifunctional sensor applications. *Prog Electromagn Res*. 2014;149:55-67.
17. Almoneef TS, Ramahi OM. Metamaterial electromagnetic energy harvester with near unity efficiency. *Appl Phys Lett*. 2015;106(15):153902.
18. Bakır M, Karaaslan M, Altıntaş O, Bagmancı M, Akdogan V, Temurtaş F. Tunable energy harvesting on UHF bands especially for GSM frequencies. *Int J Microw Wirel Technol*. 2018;10(1):67-76.
19. Bağmancı M, Karaaslan M, Altıntaş O, Karadağ F, Tetik E, Bakır M. Wideband metamaterial absorber based on CRRs with lumped elements for microwave energy harvesting. *J Microw Power Electromagn Energy*. 2018;52(1):45-59.
20. Karaaslan M, Bagmanci M, Unal E, Akgol O, Altintas O, Sabah C. Broad band metamaterial absorber based on wheel resonators with lumped elements for microwave energy harvesting. *Opt Quant Electron*. 2018;50:225.
21. Alkurt FO, Altintas O, Bakir M, et al. Octagonal shaped metamaterial absorber based energy harvester. *Mater Sci (Medžiagotyra)*. 2018;24(3):253-259.
22. Cheng Y, Nie Y, Rongzhou G. Metamaterial absorber and extending absorbance bandwidth based on multi-cross resonators. *Appl Phys B*. 2013;111(3):483-488.
23. Long C, Yin S, Wang W, Li W, Zhu J. Broadening the absorption bandwidth of metamaterial absorbers by transverse magnetic harmonics of 210 mode. *Sci Rep*. 2016;6:21431.
24. Lee HM, Lee HS. A method for extending the bandwidth of metamaterial absorber. *Int J Antennas Propag*. 2012;859429:1-7.
25. Tang J, Xiao Z, Xu K, Ma X, Wang ZJ. Polarization-controlled metamaterial absorber with extremely bandwidth and wide incidence angle. *Plasmonics*. 2016;11(5):1393-1399.
26. Mulla B, Sabah C. Multiband metamaterial absorber design based on Plasmonic resonances for solar energy harvesting. *Plasmonics*. 2016;11(5):1313-1321.
27. Chen J, Huang X, Zerihun G, Hu Z, Wang S, Wang G. Polarization-independent, thin, broadband metamaterial absorber using double-circle rings loaded with lumped resistances. *J Electron Mater*. 2015;44(11):4269-4274.
28. Ding F, Cui Y, Ge X, Jin Y, Sailing HF. Ultra-broadband microwave metamaterial absorber. *Appl Phys Lett*. 2011;100(10):103506.
29. Jaijun M, Weihong T, Kai S, Xiangyu C, Bing G. A broadband metamaterial absorber using fractal tree structure. *JPIER*. 2014;49:73-78.
30. Cheng YZ, Nie Y, Gong RZ. Design of wide-band metamaterial absorber based on fractal frequency selective and resistive films. *Phys Sci*. 2013;88:030703.
31. Karaaslan M, Bagmancı M, Unal E, Akgol O, Sabah C. Microwave energy harvesting based on metamaterial absorbers with multi-layered square split rings for wireless communications. *Opt Commun*. 2017;392:31-38.
32. Karadağ F, Çömez I, Dinçer F, Bakır M, Karaaslan M. Dynamical chiral metamaterial with Giant optical activity and constant chirality over a certain frequency band. *Appl Comput Electromagn Soc J*. 2016;31(8):919-925.
33. White, Brandon, RF To DC converter. Bradley University, Department of Electrical and Computer Engineering, Bradley University, 2016.

AUTHOR BIOGRAPHIES

MEHMET BAĞMANCI received his BSc degree from Mustafa Kemal University, Turkey in 2012. He is now working and receiving MSc at Iskenderun Technical University, Hatay, Turkey. He is the co-author of 5 scientific contributions published in international journals. His research interest includes metamaterials.

OGUZHAN AKGÖL received his BSc, MSc and PhD degrees in Electrical and Electronics Engineering from Inonu University, Turkey; Polytechnic University, Brooklyn, NY, USA and the University of Illinois at Chicago (UIC), Chicago, IL, USA respectively. He is now working at Iskenderun Technical University, Hatay, Turkey. His research interests are EM scattering, antennas and DNG materials.

MELIKŞAH ÖZAKTURK received the BSc and MSc degrees in electrical and electronic engineering from Sakarya University, Sakarya, Turkey, in 2005 and 2007, respectively, and the PhD degree from the University of Manchester, Manchester, UK, in 2012. His current research interests include renewable energy, electrical power conversion systems, electrical machines, drives and control, power electronics, wind power plants, solar power, smart grids and energy harvesting

MUHARREM KARAASLAN received the PhD degree in Physics Department from University of Cukurova, Adana, Turkey, in 2009. He has authored more than 100 research articles and conference proceedings. His research interests are applications of metamaterials, analysis and synthesis of antennas, and waveguides.

EMIN ÜNAL received his PhD degree in Electrical and Electronics Engineering from University of Gaziantep, Turkey, in 1994. He is the coauthor of about 50 scientific contributions published in international books, journals and peer-reviewed conference proceedings. His research interest includes Frequency selective surfaces and metamaterials.

MEHMET BAKIR received his Ph.D. degree in informatics department from Mustafa Kemal University in 2016. His main research interests are metamaterials, sensors, energy harvesting devices. He has authored more than 30 research articles and conference proceedings.

How to cite this article: Bağmancı M, Akgöl O, Özaktürk M, Karaaslan M, Ünal E, Bakır M. Polarization independent broadband metamaterial absorber for microwave applications. *Int J RF Microw Comput Aided Eng*. 2019;29:e21630. https://doi.org/10.1002/mmce.21630